Design of Integrable Quantum Devices

Angela Foerster[1], Karin Wittmann W.[1], Leandro Ymai[2], Daniel Grün[1], Arlei Tonel[2], Jon Links[3]

[1]Instituto de Física da UFRGS, Brazil, [2]Universidade Federal do Pampa, Brazil, [3]School of Mathematics and Physics, The University of Queensland, Australia

Abstract: The precise control of quantum systems will play a major role in the realization of atomtronic devices. Here we study models of dipolar bosons confined to 3 and 4 wells. The analysis considers both integrable and non-integrable regimes within the models. Through variation of the external field, we demonstrate how the triple-well system can be controlled between various "switched-on" and "switched-off" configurations and how the 4-well system can be controlled to generate and encode a phase into a NOON state. We discuss the physical feasibility through use of ultracold dipolar atoms in BECs (3-wells) or optical superlattices (4-wells).

Integrable Multi-Well Hamiltonians [1]

The traditional Bose-Hubbard model is not integrable (except for 2- and ∞- sites). In [1] we propose a family of integrable multi-well $(n+m)$ tunneling models. These models have additional long range interactions and in some cases (3 and 4 wells) are particular cases of the EBHM [2].

Some multi-well geometric (n,m) models:

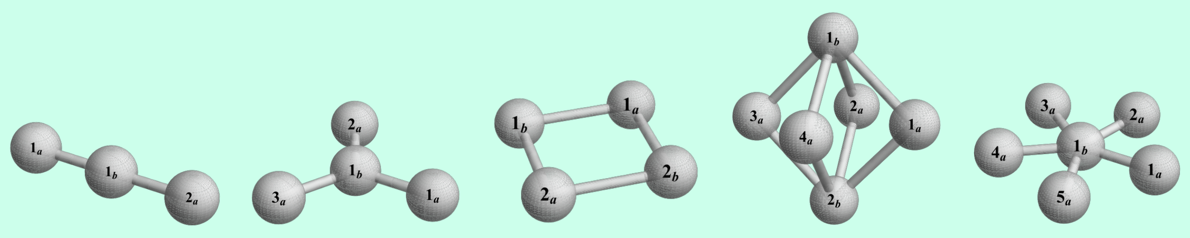

Switching device: 3-wells [3, 4]

Integrable triple well:

$$H_0 = U(N_1 - N_2 + N_3)^2 + J_1(a_1^\dagger a_2 + a_1 a_2^\dagger) + J_3(a_2^\dagger a_3 + a_2 a_3^\dagger). \qquad (1)$$

Conserved quantities: $[H_0, N] = 0, \quad [H_0, Q] = 0, \quad [N, Q] = 0, \quad Q = J_1^2 N_3 + J_3^2 N_1 - J_1 J_3(a_1^\dagger a_3 + a_3^\dagger a_1)$

The charge Q provides an H_{eff} which, in the resonant regime $(UN/J >> 1)$ yields analytical formulae.

This model is a particular integrable case of the system for dipolar bosons (EBHM) presented in [2]:

$$\mathcal{H} = \frac{U_0}{2}\sum_{i=1}^{3} N_i(N_i - 1) + \sum_{i=1}^{3}\sum_{j=1, j\neq i}^{3} \frac{U_{ij}}{2} N_i N_j + J_1(a_1^\dagger a_2 + a_1 a_2^\dagger) + J_3(a_2^\dagger a_3 + a_2 a_3^\dagger).$$

as long as the integrability condition $U_{13} = U_0$ is satisfied. Also $U_{12} = U_{23} = \alpha U_{13}$, where $4 \le \alpha \le 8$ depends on the geometry of the trap and $U = (\alpha - 1)U_0/4$.

Breaking the Integrability

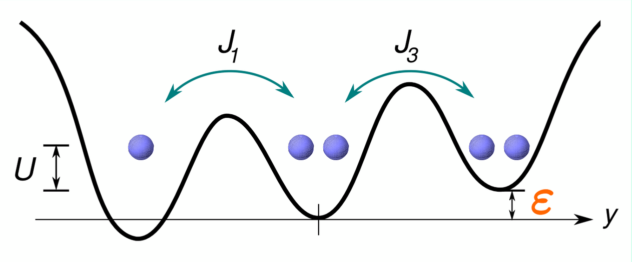

$H = H_0 + \varepsilon\,(N_3 - N_1)$ ε : external field $\quad [H, Q] \neq 0$

Quantum dynamics:

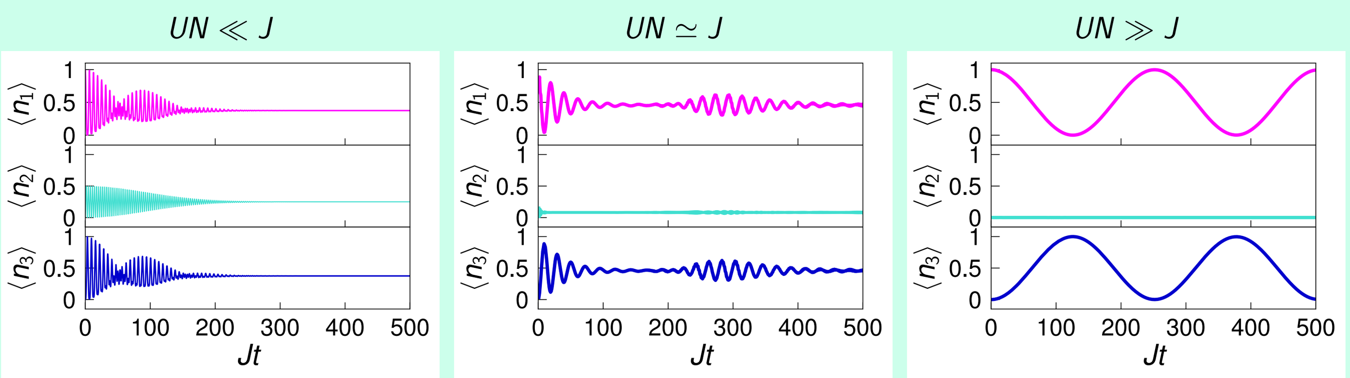

Time evolution of expectation values. N=60, $J=1$, $\varepsilon=0$, U=0.001, 0.015 and 0.17.
Tunneling through the gate is switched-off: resonant

Control of resonant tunneling:

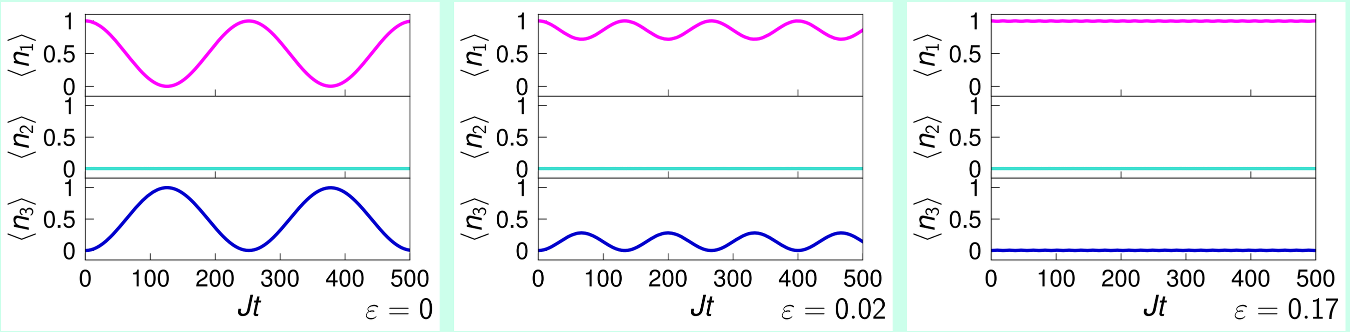

Time evolution of expectation values. N=60, $J=1$, U=0.17, ε=0, 0.02 and 0.17.
By applying the external field ε the tunneling amplitude between wells 1 and 3 and the frequency ω can be controlled while $< n_2 >$ remains negligible.

Analytical expressions: (semi-classical analysis)

$$\omega = \frac{2\lambda J_1 J_3}{\sqrt{\Delta n}} \qquad \Delta n = \frac{1}{(1+\gamma^2)} \qquad \gamma = \frac{(\lambda(J_1^2 - J_3^2) - 2\varepsilon)}{2\lambda J_1}$$

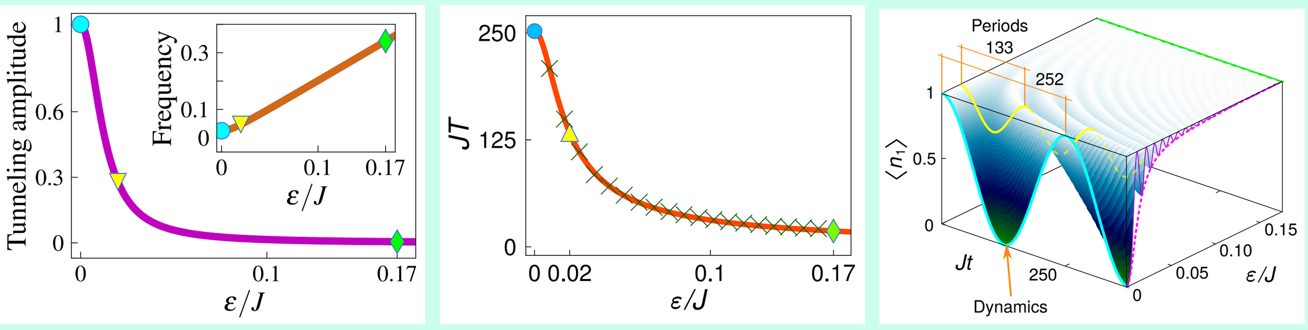

Tunnel Amplitude (Δn) vs. ε Period (T) vs. ε $\langle n_1\rangle$ Dynamics vs. ε

Physical feasibility:

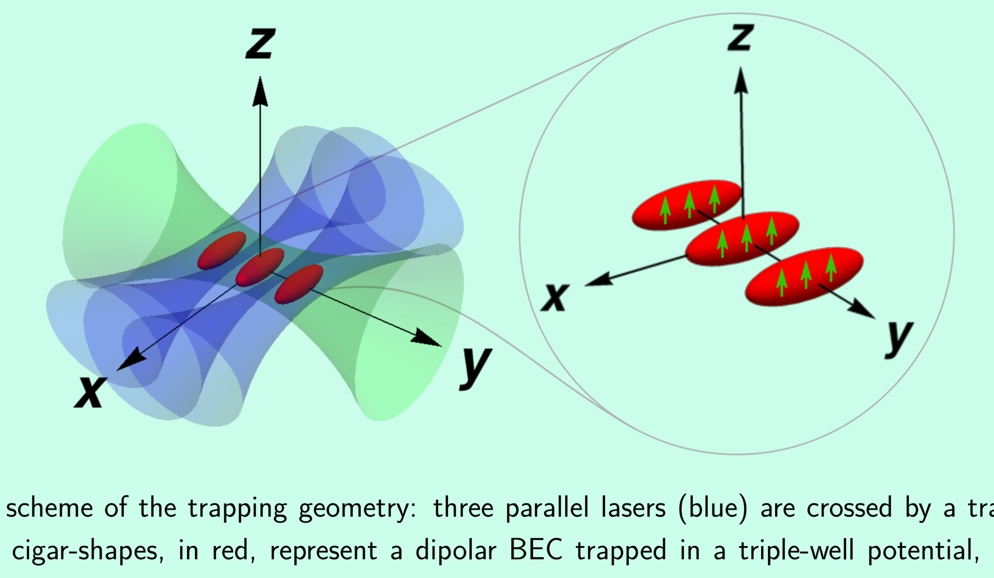

Experimental scheme of the trapping geometry: three parallel lasers (blue) are crossed by a transverse beam (green). The cigar-shapes, in red, represent a dipolar BEC trapped in a triple-well potential, and the green internal arrows depict the orientation of the dipoles. The transverse beam performs the function of the external field that controls the device. Its focus, when slowly displaced along the y-axis by Δy changes the tilting of wells 1 and 3 (breaking).

NOON states: 4-wells [5, 6]

Integrable Extended Bose-Hubbard Model (EBHM):

$$H = \frac{U_0}{2}\sum_{i=1}^{4} N_i(N_i - 1) + \sum_{i=1}^{4}\sum_{j=1, j\neq i}^{4} \frac{U_{ij}}{2} N_i N_j - \frac{J}{2}[(a_1^\dagger + a_3^\dagger)(a_2 + a_4) + (a_1 + a_3)(a_2^\dagger + a_4^\dagger)], \qquad (2)$$

An integrable 4-wells model [1] can be obtained from EBHM [2] as long as it complies with the integrability condition $U_0 = U_{13} = U_{24}$ and $U_{12} = U_{23} = U_{34} = U_{14}$.

Conserved quantities: $[H, N] = [H, Q_k] = [N, Q_k] = 0$, $k = 1, 2$. The charges Q_1, Q_2 provide an H_{eff} which, in the resonant regime $U|M - P| \gg J$, yields analytical formulae. Here $U = (U_{12} - U_0)/4$.

NOON-state Protocols:

We describe two protocols that enable the generation of NOON states. For Protocol I the outcomes are probabilistic while Protocol II are deterministic. Both protocols consider the initial state $|\Psi_0\rangle = |M, P, 0, 0\rangle$ and are built around a general time evolution operator: $(\mu, \nu$: applied fields)

$$\mathcal{U}(t, \mu, \nu) = \exp\left(-\frac{it}{\hbar}[H + \mu(N_2 - N_4) + \nu(N_1 - N_3)]\right)$$

It is convenient to introduce the phase variable $\theta = 2\mu t_\mu/\hbar$, and to fix $t_\nu = \hbar\pi/(4M\nu)$.

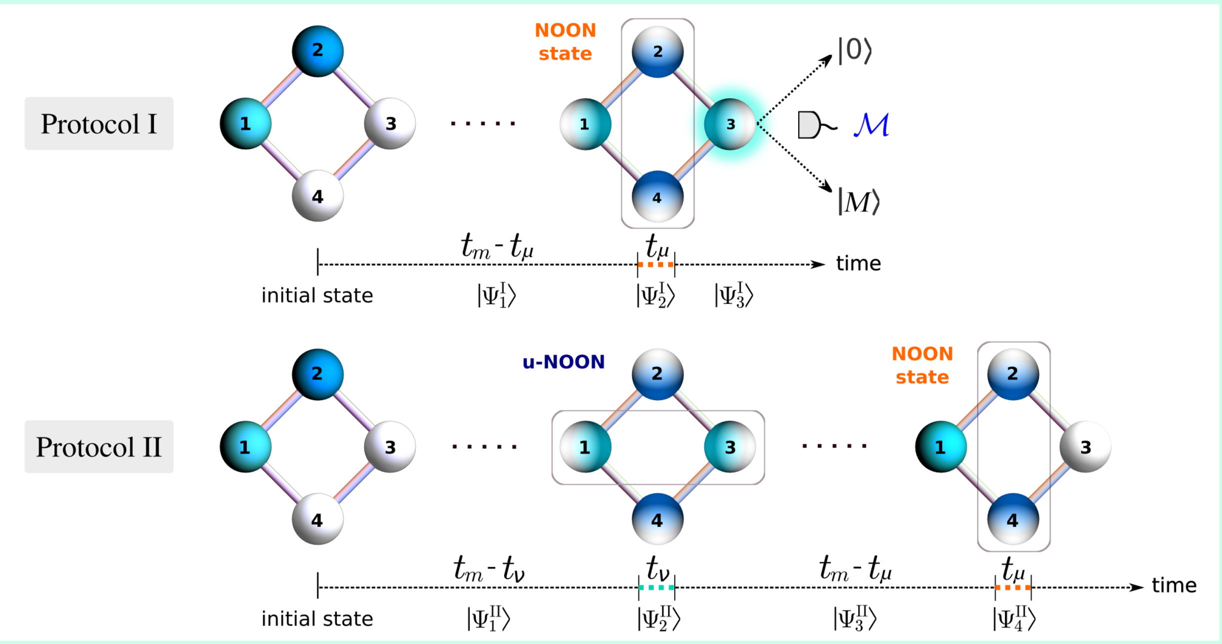

Protocol I

Here we employ breaking of integrability through an applied field $\mu(N_4 - N_2)$ to subsystem $B = \{2, 4\}$ and a measurement process $\mathcal{M}$:

(i) $|\Psi_1^{\mathrm{I}}\rangle = \mathcal{U}(t_m - t_\mu, 0, 0)\,|\Psi_0\rangle$;
(ii) $|\Psi_2^{\mathrm{I}}\rangle = \mathcal{U}(t_\mu, \mu, 0)\,|\Psi_1^{\mathrm{I}}\rangle$;
(iii) $|\Psi_3^{\mathrm{I}}\rangle = \mathcal{M}\,|\Psi_2^{\mathrm{I}}\rangle$,

where $\mathcal{M} = 0, M$ represents a projective measurement of the number of bosons at site 3 which heralds a high-fidelity NOON state in subsystem B and $t_m = \hbar\pi/(2\Omega)$, with $\Omega = J^2/(4U((M-P)^2 - 1))$.
In an idealized limit $t_\mu \to 0$, $\mu \to \infty$, with $\beta = (-1)^{(N+1)/2}$

$$|\Psi_3^{\mathrm{I}}\rangle = \begin{cases} \frac{1}{\sqrt{2}}\left(\beta\,|M, P, 0, 0\rangle + e^{iP\theta}\,|M, 0, 0, P\rangle\right), & r = 0, \\ \frac{1}{\sqrt{2}}\left(|0, P, M, 0\rangle - \beta e^{iP\theta}\,|0, 0, M, P\rangle\right), & r = M, \end{cases} \qquad (3)$$

These states are recognized as products of a NOON state for subsystem $B = \{2, 4\}$ with Fock basis states for subsystem $A = \{1, 3\}$.

Protocol II

Here the following sequence of steps are implemented to arrive at a NOON state in subsystem $B = \{2, 4\}$ and deterministic state in subsystem $A = \{1, 3\}$:

(i) $|\Psi_1^{\mathrm{II}}\rangle = \mathcal{U}(t_m - t_\nu, 0, 0)\,|\Psi_0\rangle$;
(ii) $|\Psi_2^{\mathrm{II}}\rangle = \mathcal{U}(t_\nu, 0, \nu)\,|\Psi_1^{\mathrm{II}}\rangle$;
(iii) $|\Psi_3^{\mathrm{II}}\rangle = \mathcal{U}(t_m - t_\mu, 0, 0)\,|\Psi_2^{\mathrm{II}}\rangle$;
(iv) $|\Psi_4^{\mathrm{II}}\rangle = \mathcal{U}(t_\mu, \mu, 0)\,|\Psi_3^{\mathrm{II}}\rangle$.

where ν represent the breaking of integrability through an applied field $\nu(N_3 - N_1)$ to subsystem $A = \{1, 3\}$.
In an idealized limit $\mu, \nu \to \infty$, $t_\mu, t_\nu \to 0$, with $\Upsilon = \beta\exp(i(P\theta - \pi/2))$,

$$|\Psi_4^{\mathrm{II}}\rangle = \frac{1}{\sqrt{2}}\Big(|M, P, 0, 0\rangle + \Upsilon\,|M, 0, 0, P\rangle\Big) \qquad (4)$$

Fidelity and Readout probabilities:

We give numerical simulations of the protocols to show that, for physically realistic settings where the fields are applied for finite times, high-fidelity outcomes for NOON state production persist. The fidelities are computed:

$$F_{\mathrm{I}} = |\langle\Psi_3^{\mathrm{I}}|\Phi_3^{\mathrm{I}}\rangle| > 0.9 \qquad F_{\mathrm{II}} = |\langle\Psi_4^{\mathrm{II}}|\Phi_4^{\mathrm{II}}\rangle| > 0.9$$

where $|\Psi\rangle$ denotes the analytical states and $|\Phi\rangle$ the numerically state obtained by EBHM (2) time evolution. As the values remain almost constant for $P\theta \in [0, \pi]$, varying less than 1%, we display here only one case

	F_{I}		F_{II}	$P\theta = \pi/2$		
	$r=0$	$r=M$		t_μ	t_ν	t_m
Set 1	0.986	0.997	0.974	0.0024 s	0.0065 s	6.1639 s
Set 2	0.964	0.991	0.920	0.0026 s	0.0072 s	2.8913 s

Table 1: Fidelities for Protocols I and II. Numerical calculations for $M = 4$ and $P = 11$.

Set 1: $\{U/\hbar = 104.85,\ J/\hbar = 71.62,\ \mu/\hbar = 30.02\}$ (in Hz)
Set 2: $\{U/\hbar = 105.60,\ J/\hbar = 104.95,\ \mu/\hbar = 27.42\}$ (in Hz)

A means to test the reliability of the system, through a statistical analysis of local measurement outcomes is directly built into the design. For both protocols, once the output state has been attained we can continue to let the system evolve under $\mathcal{U}(t_m, 0, 0)$. This yields the readout states that can be obtained analytically

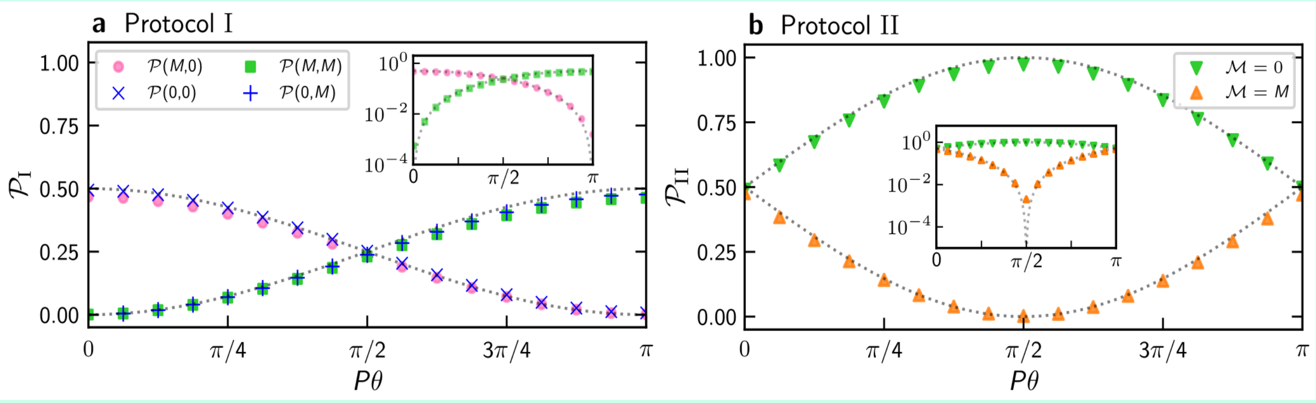

Readout probabilities for Protocols I and II. Comparison between analytic and numerically-calculated probabilities for parameters of Set 1 for different values of $P\theta$

Physical feasibility:

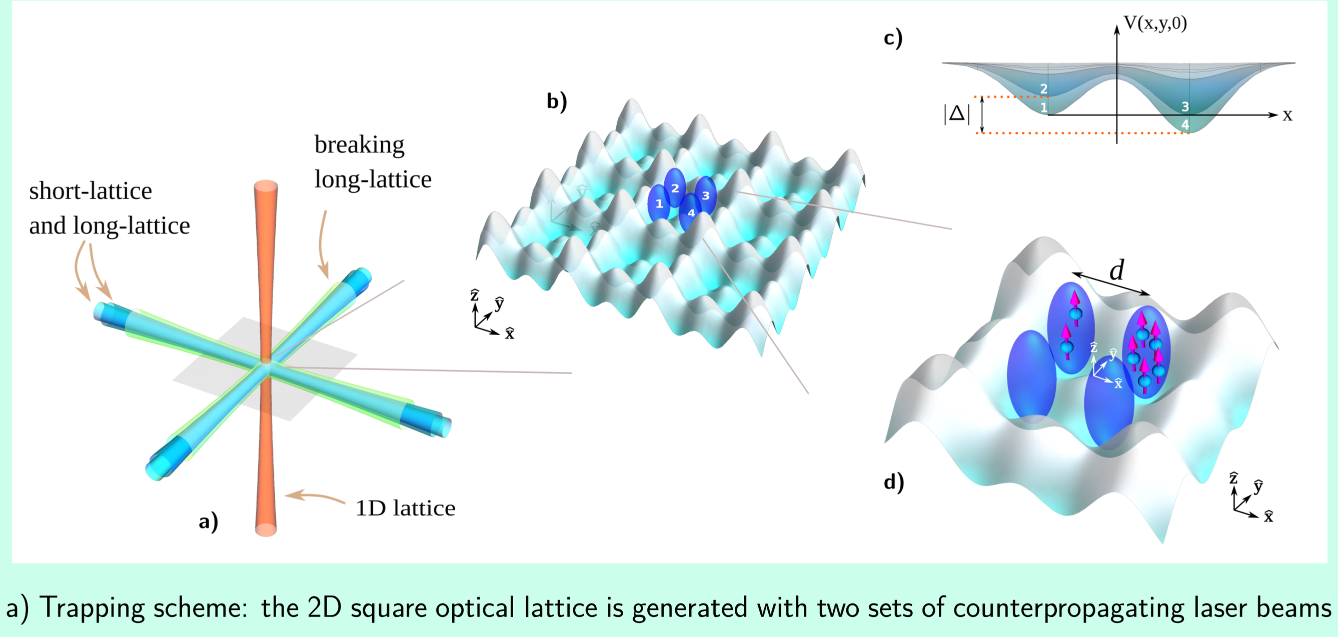

a) Trapping scheme: the 2D square optical lattice is generated with two sets of counterpropagating laser beams crossing at 90° with the other. The superlattice of four-site model is achieved overlapping the 2D short-lattice (cyan) and long-lattice (blue). The vertical lattice (orange) provides confinement in z direction. An additional 2D square long-lattice (green) is used to implement the integrability break control. b) Zoom into the region of the superlattice which contains the four-site plaquette. c) Breaking-of-integrability scheme. The system's integrability can be broken by changing the phase difference between the superlattice and the additional 2D square long-lattice, effectively causing a potential imbalance Δ between wells 1 and 3.

References

[1] L. Ymai et al, J. Phys. A50, 2017.
[2] T. Lahaye et al, Phy. Rev. Lett. 104, 2010.
[3] K. Wittmann et al, Communications Physics 1 (1) , 2018.
[4] A. Tonel et al, SciPost Phys. Core 2 (003), 2020.
[5] D. Grun et al, arXiv preprint arXiv:2004.11987.
[6] D. Grun et al, arXiv preprint arXiv:2102.02944.

Contact Information: angela@if.ufrgs.br

Bose-Einstein Condensation 2021, September 11 to 17, 2021